JUSTC

Letter

http://justc.ustc.edu.cn

Received: November 17, 2021; Accepted: February 09, 2022

Experimental investigation of quantum discord in DQC1

Tingwei Li[1], Yang Wu[1,2], Fangzhou Jin[3] ✉, and Xing Rong[1,2] ✉

[1]*CAS Key Laboratory of Microscale Magnetic Resonance and School of Physical Sciences, University of Science and Technology of China, Hefei 230026, China;*

[2]*CAS Center for Excellence in Quantum Information and Quantum Physics, University of Science and Technology of China, Hefei 230026, China;*

[3]*Department of Fundamental Subjects, Wuchang Shouyi University, Wuhan 430064, China*

✉Correspondence: Fangzhou Jin, E-mail: fzjin@wsyu.edu.cn; Xing Rong, E-mail: xrong@ustc.edu.cn

Graphical abstract

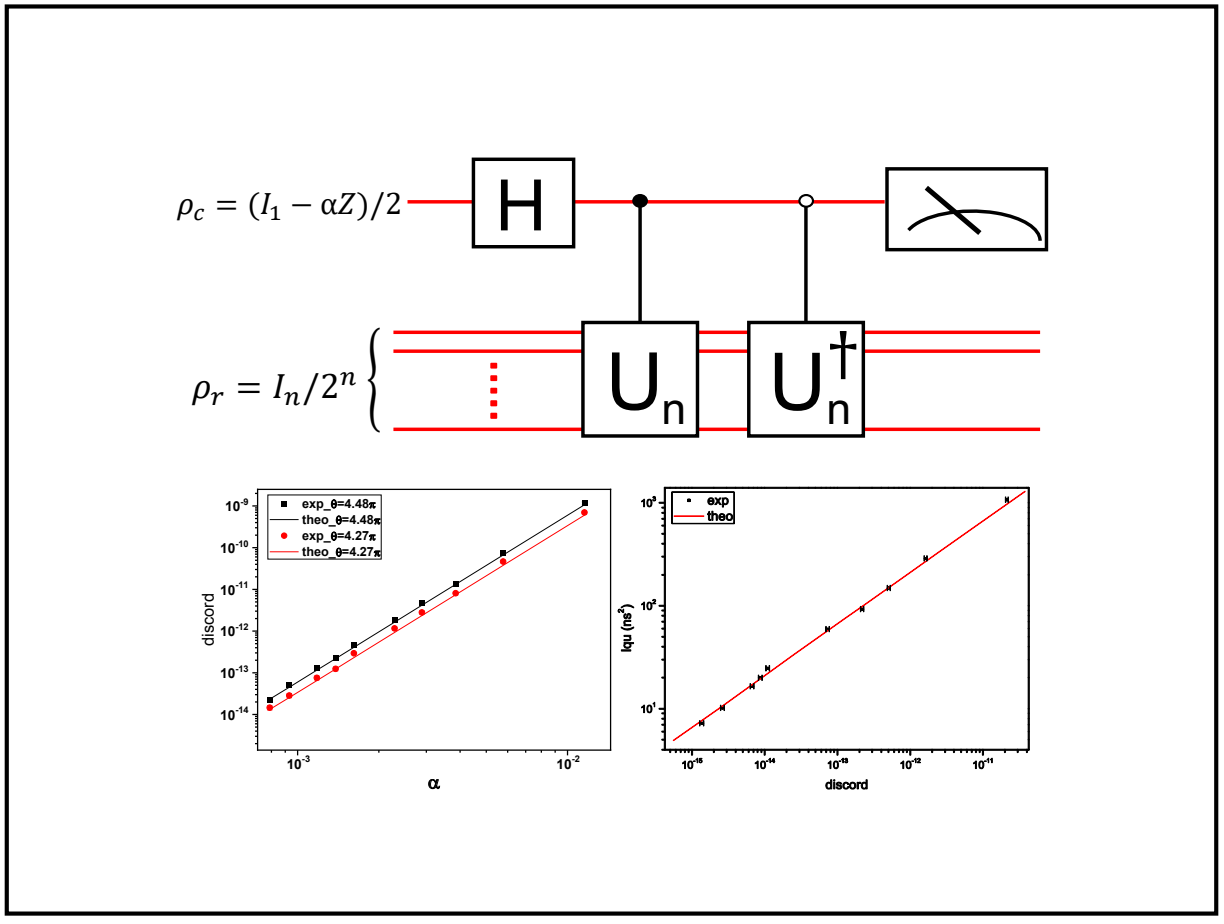

Quantum circuit of DQC1 algorithm and experimental results.

Public summary

■ DQC1 algorithm is implemented in a solid system in a real noisy environment.

■ Nonvanishing quantum discord is observed.

■ Quantum discord is responsible for the power of DQC1.

Citation: Li T W, Wu Y, Jin F Z, et al. Experimental investigation of quantum discord in DQC1. *JUSTC*, **2022**, 52(4): 2. DOI: 10.52396/JUSTC-2021-0267

JUSTC

Letter

http://justc.ustc.edu.cn

Received: November 17, 2021; Accepted: February 09, 2022

Experimental investigation of quantum discord in DQC1

Tingwei Li[1], Yang Wu[1,2], Fangzhou Jin[3] ✉, and Xing Rong[1,2] ✉

[1]*CAS Key Laboratory of Microscale Magnetic Resonance and School of Physical Sciences, University of Science and Technology of China, Hefei 230026, China;*

[2]*CAS Center for Excellence in Quantum Information and Quantum Physics, University of Science and Technology of China, Hefei 230026, China;*

[3]*Department of Fundamental Subjects, Wuchang Shouyi University, Wuhan 430064, China*

✉Correspondence: Fangzhou Jin, E-mail: fzjin@wsyu.edu.cn; Xing Rong, E-mail: xrong@ustc.edu.cn

Cite This: *JUSTC*, **2022**, 52(4): 2 (6pp)

Read Online

Abstract: Quantum discord has been proposed as a resource responsible for the exponential speedup in deterministic quantum computation with one pure qubit (DQC1). Investigation of the quantum discord generated in DQC1 is of significant importance from a fundamental perspective. However, in practical applications of DQC1, qubits generally interact with the environment. Thus, it is also important to investigate the discord when DQC1 is implemented in a noisy environment. We implement DQC1 on an electron spin resonance (ESR) architecture in such an environment and nonzero quantum discord is observed. Furthermore, we find that the values of discord correspond to the values of purity α and quantum Fisher information, which reflect the power of the algorithm. Our results provide further evidence for the role of discord as a resource in DQC1 and are beneficial for understanding the origin of the power of quantum algorithms.

Keywords: quantum discord; electron spin resonance; DQC1

CLC number: O413.1 **Document code:** A

Most quantum computation algorithms require qubits prepared in a pure initial state[1, 2], whereas the mixed state is more naturally accessible for many experimental candidates for quantum computation. Thus, it has attracted considerable interest since mixed-state quantum computation was proposed[3–7]. A typical mixed-state quantum computation model is DQC1, deterministic quantum computation with one pure qubit[8]. Unlike pure-state quantum computation, in which the generation of a large amount of entanglement is necessary for exponential speedup[9, 10], entanglement is at most marginally observed in DQC1[11, 12]. Thus, a fascinating and fundamental question arises: what is responsible for the speedup of DQC1?

It has been pointed out that entanglement cannot describe all the nonclassical features in the correlations[13], whereas quantum discord can be used as a measurement of the quantumness of correlations[14–16]. Thus, discord has been proposed as a figure of merit for characterizing the resources in DQC1[17], and it has been extensively researched[18–21]. Quantum discord has also been demonstrated to be a resource for encoding information and remote state preparation[22, 23], implying a similar role of discord in DQC1. Nonvanishing quantum discord has been experimentally detected in DQC1[24–27]. However, since it has been proven that almost all quantum states have nonzero discord[28], the observation of nonvanishing discord presents insufficient evidence for the role of discord. The relationship between the discord and purity of the control qubit in DQC1 has been analyzed[17]. However, to date, no experimental demonstration has been implemented.

In addition to the fascinating properties from a fundamental perspective, DQC1 realizes an exponential speedup over the best known classical algorithm for specific tasks and has been used in a variety of fields such as quantum metrology[29], thermodynamics[30], calculation of fidelity decay[31], and estimating Jones and polynomials[32]. When the DQC1 algorithm is implemented in practical applications, the system inevitably interacts with the environment. The interaction usually causes a non-unitary evolution of the system, making an unideal implementation of the algorithm. It is also important to detect and observe the behavior of quantum discord in this case, since if discord is the resource advancing the speedup of DQC1, it should also be responsible for the practical implementation in a real environment as long as the implementation is successful. This is particularly important when considering the practical applications of DQC1.

In this study, the DQC1 algorithm is implemented in a solid system in a real noisy environment. The normalized trace of U_n^2 is estimated using the free evolution under the system Hamiltonian, where U_n denotes a quantum gate. Although the interaction between the system and environment causes a decay of the algorithm output, the algorithm can be successfully implemented, and nonvanishing quantum discord is observed for $\theta \neq k\pi$, θ is a parameter related to the hyperfine coupling and evolutionary time, though the discord decays by approximately two orders of magnitude owing to the interaction. This demonstrates a successfully implemented DQC1 algorithm in a real noisy environment, in which nonzero quantum discord is present and potentially plays an important role. Furthermore, we detect the quantum discord generated in the algorithm for different values of purity α of the control

DOI: 10.52396/JUSTC-2021-0267

JUSTC, **2022**, 52(4): 2

qubit. Since a smaller value of α requires more runs of the algorithm for a fixed accuracy of the estimation (see the text below for details), the variation in α represents a variation in the algorithm power. Our results show that the value of quantum discord corresponds to the value of α, indicating that there is more discord generated in the more powerful algorithm. The implementation can be immediately used to estimate the hyperfine coupling of the electron and nuclear spin without modification. The quantum Fisher information places an upper bound on the estimation precision[33–35] and also reflects the power of the algorithm. We analyze the relationship between the quantum Fisher information and quantum discord when varying α and find an increasing function of the quantum Fisher information with respect to increasing quantum discord. This implies that larger amounts of discord can lead to a more precise estimation, and thereby, reflecting that the algorithm is more powerful. All the results indicate that quantum discord is responsible for the power of DQC1. Although insufficient, our results provide strong evidence of the role of quantum discord as a resource in DQC1.

Fig. 1 shows the quantum circuit of the DQC1 algorithm for estimating the normalized trace of U_n^2, in which U_n is a n-qubit quantum gate. The required input state consists of a single control qubit c, whose density matrix is $\frac{1}{2}(I_1 - \alpha Z)$, and a register of n qubits in the completely mixed state $I_n/2^n$, where α reflects the purity of the qubit, I_n denotes the n-qubit identity, and Z denotes the Pauli-z matrix. The circuit consists of a standard Hadamard gate on the control qubit c and two controlled-gates. Among the two gates, the first gate leads to a unitary evolution U_n, which is applied to the register if and only if qubit c is in the logical state of $|1\rangle$, and the second corresponds to unitary $U_n^\dagger$ on the register when c is in the state $|0\rangle$, where $U_n^\dagger$ denotes the Hermitian conjugate of U_n. The complete evolution of the two controlled-gates can be described as

$$U_{ct} = \begin{pmatrix} U_n^\dagger & 0 \\ 0 & U_n \end{pmatrix} \tag{1}$$

After the evolution the output state of all $n+1$ qubits can be expressed as

$$\rho_{cr} = \frac{1}{2N}\begin{pmatrix} I_n & -\alpha U_n^{\dagger 2} \\ -\alpha U_n^{\ 2} & I_n \end{pmatrix} \tag{2}$$

where $N = 2^n$. By performing a partial trace over the register, the reduced state of qubit c can be obtained as

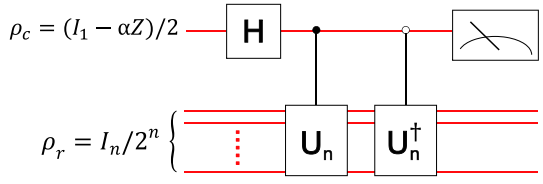

Fig. 1. DQC1 algorithm to estimate the normalized trace of U_n^2. I_n is the n-qubit identity, α reflects the degree of purity of control qubit c, and Z denotes the Pauli operator Z. The normalized trace $\mathrm{Tr}(U_n^2)/2^n$ can be derived from the expectation values of the output of qubit c measured on the Pauli X and Y bases.

$$\rho_c = \frac{1}{2}\begin{pmatrix} 1 & -\alpha[\mathrm{Tr}(U_n^2)]^*/N \\ -\alpha\mathrm{Tr}(U_n^2)/N & 1 \end{pmatrix} \tag{3}$$

The normalized trace of $U_n^{\ 2}$ can be retrieved by measuring the expectation values of the standard Pauli operators X and Y on the output state of qubit c, since $\langle X\rangle = -\alpha\mathrm{Re}[\mathrm{Tr}(U_n^{\ 2})/N]$ and $\langle Y\rangle = -\alpha\mathrm{Im}[\mathrm{Tr}(U_n^{\ 2})/N]$. It should be noted that a small value of α leads to small absolute values of $\langle X\rangle$ and $\langle Y\rangle$, thereby making it more difficult to estimate the normalized trace. It is evident that for a fixed accuracy, a smaller α implies more runs of the algorithm considering the same U_n, and thereby, indicating less power of the algorithm.

We implement the first-order case ($n = 1$) on an electron spin resonance(ESR) architecture. The E_2' center in α-quartz[36–41], which consists of an electron trapped near the Si atom and a proton localized on the O vacancy, is used as the system. The electron spin and proton nuclear spin provide control and register qubits, respectively. Fig. 2a shows the continuous wave ESR spectrum of the E_2' center recorded at room temperature with the optical axis of quartz oriented along the magnetic field. The split of the two peaks presents the hyperfine coupling of the electron and nuclear spins. The static Hamiltonian can be expressed as

$$H_0 = \omega_S S_z + \omega_I I_z + 2\pi A S_z I_z \tag{4}$$

where $\omega_S = g\beta B_0/\hbar$ and $\omega_I = -g_n\beta_n B_0/\hbar$ characterize the Zeeman interactions for the electron and nuclear spins, respectively, and A (1.12 MHz at room temperature) describes the hyperfine coupling. The initial state is thermal state with a density matrix $\rho_{th} = \mathrm{e}^{-H_0/kT}/\mathrm{Tr}(\mathrm{e}^{-H_0/kT})$, where T denotes the temperature. Given that ω_S is approximately three orders of magnitude larger than ω_I and A and $\hbar\omega_S$ is approximately two to three orders less than kT within the experimental temperat-

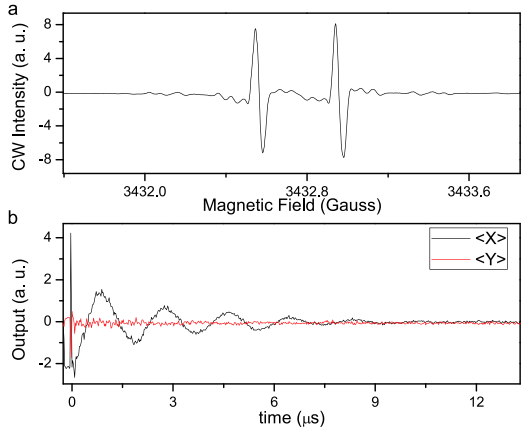

Fig. 2. (a) Continuous wave (CW) ESR spectrum of the E_2' center in α-quartz recorded at room temperature with the optical axis of the quartz oriented along the magnetic field. The split of the two peaks indicates the hyperfine coupling of the electron and nuclear spins. (b) Output of algorithm as evolution time varies for temperature $T = 80$ K. Temperature T and evolution time t represent α and θ, respectively, as described in the text. The output value is not normalized. The area with time $t < 0$ is related to the single-qubit gate on the control qubit. The output near $t = 0$ is affected by the protection pulse, and thus it differs from the actual value of the output. The decay of the output originates from the interaction with the environment during the evolution of the system, as described in the text.

DOI: 10.52396/JUSTC-2021-0267
JUSTC, **2022**, 52(4): 2

ure range, the thermal state can be approximated as

$$\rho_{th} = \frac{1}{2}(I_1 - \alpha Z) \otimes \frac{1}{2} I_1 \tag{5}$$

where

$$\alpha = \hbar\omega_s/(2kT) \tag{6}$$

For the initial state, the Hadamard gate on the control qubit is identical to a $\pi/2$ rotation of the qubit along the y axis. Unlike the optical implementation of DQC1[24], in which the two-qubit controlled-gate is realized non-deterministically, the two-qubit gates are implemented deterministically via the free evolution of the system. In a double-rotating frame, the system Hamiltonian under free evolution is

$$H = 2\pi A S_z I_z \tag{7}$$

The evolution can be described with the operator

$$U_{ct} = \begin{pmatrix} e^{-i2\pi At/4} & 0 & 0 & 0 \\ 0 & e^{i2\pi At/4} & 0 & 0 \\ 0 & 0 & e^{i2\pi At/4} & 0 \\ 0 & 0 & 0 & e^{-i2\pi At/4} \end{pmatrix} \tag{8}$$

which gives

$$U_1 = \begin{pmatrix} e^{i\theta/4} & 0 \\ 0 & e^{-i\theta/4} \end{pmatrix} \tag{9}$$

with

$$\theta = 2\pi At \tag{10}$$

However, the practical evolution of the system becomes non-unitary due to interaction with the environment. This leads to an exponential decay in the off-diagonal elements of the density matrix under evolution. Thus, the practical output state $\rho_{cr,p}$ deviates from the output state ρ_{cr} of the perfect algorithm circuit.

$$\rho_{cr,p} = \frac{1}{4}\begin{pmatrix} I_1 & -\alpha U_1^{\dagger 2} e^{-t/T_2^*} \\ -\alpha U_1{}^2 e^{-t/T_2^*} & I_1 \end{pmatrix} \tag{11}$$

where T_2^* (3.3 μs at room temperature) denotes the dephasing time of the electron spin. The outputs $\langle X\rangle$ and $\langle Y\rangle$ also decay by a factor of e^{-t/T_2^*}. The algorithm can still be successfully implemented to estimate the normalized trace because the deterministic decay can be compensated.

Fig. 2b shows the practical output of the algorithm as the evolution time varies at $T = 80$ K. The value of the output is not normalized. The area, where $t < 0$, only records the implementation of the one-qubit gate before evolution, and thus, is not the algorithm output. The deviation of the output near $t = 0$ is due to the influence of the protection pulse. The output presents an overall decay in accordance with the theoretical analysis above.

To analyze the generated quantum discord, quantum state tomography[42] is used to reconstruct the density matrix ρ_{cr} of the two-qubit output state. The mutual information for ρ_{cr} is $I(\rho_{cr}) = S(\rho_c) + S(\rho_r) - S(\rho_{cr})$, where $S(\rho) = -\mathrm{Tr}(\rho \log_2 \rho)$ is von Neumann entropy. The classical correlation can be obtained using the maximum accessible information about register qubit r when performing a conditional positive-operator-valued measurement $\{\Pi_k\}$ on qubit c, i.e., $C_c(\rho_{cr}) = \max_{\{\Pi_k\}}[S(\rho_r) - \sum_k p_k S(\rho_{r|\Pi_k})]$, where $p_k = \mathrm{Tr}(\Pi_k \rho_{cr} \Pi_k^\dagger)$ and $\rho_{r|\Pi_k} = \mathrm{Tr}_c(\Pi_k \rho_{cr} \Pi_k^\dagger)/p_k$. The difference between the mutual information and classical correlation gives quantum discord $D_c(\rho_{cr}) = I(\rho_{cr}) - C_c(\rho_{cr})$.

Figs. 3a and 3b show the experimentally detected quantum discord as θ varies for $T = 20$ K (corresponding to $\alpha = 1.16\times10^{-2}$) and $T = 80$ K (corresponding to $\alpha = 2.89\times10^{-3}$). Nonzero quantum discord are observed for both α when $\theta \neq k\pi$ for integer k. The overall decay of discord is due to the interaction with environment during the evolution of the system. When considering the effect of the interaction, i.e., with Eq. (11), the theoretical predicted quantum discord fits the experimental data extremely well. In Figs. 3c and 3d, we compensate the decay of off-diagonal elements of the reconstructed density matrices by multiplying e^{t/T_2^*}, and we calculate quantum discord with the compensated density matrices. As expected, after compensating the decay, the quantum discord varies periodically with θ while the overall decay feature disappears. The results are in good agreement with theoretical predictions considering perfect circuit operations(i.e., based on Eq. (2)). Although practically detected quantum discord is approximately two orders smaller than that calculated with compensated density matrices, it is still nonzero in the successfully implemented algorithm.

Fig. 4 shows the relationship between quantum discord and α (or temperature T). In Fig. 4a, the variation in experimentally detected quantum discord with temperature is depicted for fixed $\theta = 4.48\pi$ and $\theta = 4.27\pi$. In both cases, the quantum discord decreases as the temperature increases. By considering the relationship between the temperature and α, it is clear that the discord increases as α increases. Since the quantum discord is significantly influenced by the interaction of the system and environment, we also calculate the discord with compensated density matrices in Fig. 4b for $\theta = 4.48\pi$. The

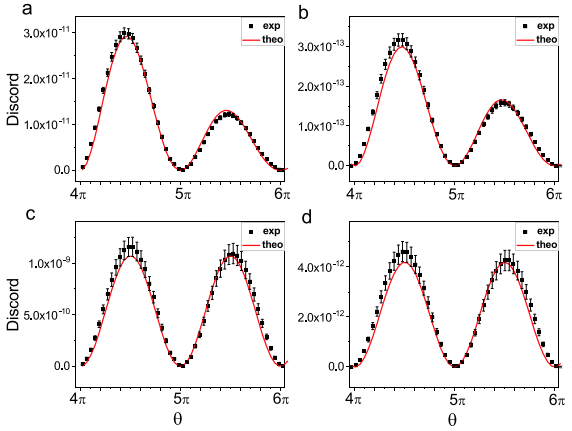

Fig. 3. Quantum discord generated for: (a)(c) $T = 20$ K ($\alpha = 1.16\times10^{-2}$), and (b)(d) $T = 80$ K ($\alpha = 2.89\times10^{-3}$). In (a) and (b), the experimental data (black square points) are practically detected, quantum discord is calculated with the original reconstructed density matrices of the output state, and the theoretical predictions (red curves) are calculated using Eq. (11) considering the interaction of the system with the environment. In (c) and (d), the experimental data (black square points) are calculated using the compensated density matrices, as described in the text, and the theoretical predictions (red curves) are calculated using Eq. (2) for perfect algorithm circuit operation. The error bars include only the estimated errors in numerically calculating quantum discord with density matrices.

DOI: 10.52396/JUSTC-2021-0267
JUSTC, **2022**, 52(4): 2

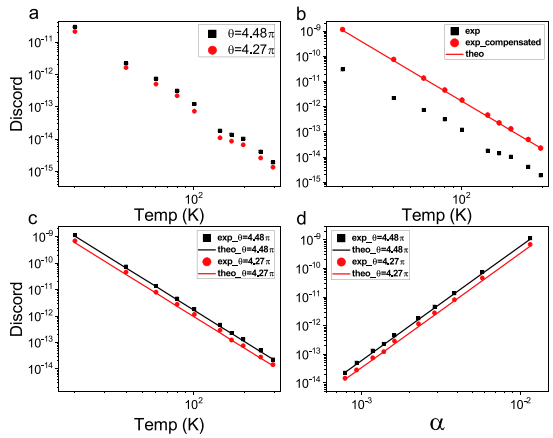

Fig. 4. (a) Experimentally detected quantum discord with varying temperature for $\theta = 4.48\pi$ (black squares) and $\theta = 4.27\pi$ (red dots). Discord is calculated with the original reconstructed density matrices of the output state. (b) Comparison of quantum discord calculated using the original (black squares) and compensated (red dots) density matrices for $\theta = 4.48\pi$. The theoretical predictions (red curve) are calculated using Eq. (2) for perfect circuit operation. (c) Quantum discord calculated using compensated density matrices with varying temperature for $\theta = 4.48\pi$ (black squares) and $\theta = 4.27\pi$ (red dots). The theoretical predictions (black and red curves) are calculated using Eq. (2) for perfect circuit operation. (d) Same as (c), but for quantum discord with varying α. α and the temperature is related one-to-one according to Eq. (6). Error bars only include the estimated errors for numerical calculation of the quantum discord with density matrices, and are covered by symbols of points.

calculated quantum discord with compensated density matrices is in good agreement with the theoretical prediction calculated with Eq. 2 for perfect circuit operation. The difference between the discord calculated with original and compensated density matrices is approximately two orders, and this shows the decay of discord due to the interaction with the environment during the system evolution corresponding to θ from 0 to 4.48π. Fig. 4c compares the quantum discord calculated with compensated density matrices and theoretical predictions for perfect circuit operation. A good agreement is realized for both $\theta = 4.48\pi$ and $\theta = 4.27\pi$. In Fig. 4d, the varying temperature is translated to varying α, and the relationship between quantum discord (calculated with compensated density matrices) and α is clearly presented. It shows that the value of quantum discord corresponds to the value of α. Given that larger α implies a more powerful DQC1 algorithm, in this case, the more powerful algorithm generates larger amounts of quantum discord.

As $\theta = 2\pi At$ (Eq. (10)), our implementation of the DQC1 algorithm can be immediately used to estimate the hyperfine coupling A. Supposing that $\rho(A)$ denotes the output density matrix which contains the parameter A, the precision of estimating A after a measurement $E(\xi)$ on the output state is bounded by the Fisher information $F(A) = \int \mathrm{d}\xi \frac{1}{p(\xi|A)} \left(\frac{\partial p(\xi|A)}{\partial A}\right)^2$, where $p(\xi|A) = Tr[E(\xi)\rho(A)]$ is the probability distribution of the measurement result ξ. The quantum Fisher information is the maximum of the Fisher information over all measurements $E(\xi)$, i.e., $Iqu(A) = \max_{\{E(\xi)\}} F(A)$. Thus, the quantum Fisher information places an upper bound on estimation precision. By optimizing the measurement, the quantum Fisher information can be derived as $Iqu = Tr[\rho' \mathcal{L}_\rho(\rho')]$, where $\rho' = \frac{\mathrm{d}\rho}{\mathrm{d}A}$ and $\mathcal{L}_\rho(O) = \sum_{\{j,k|p_j+p_k\neq 0\}} \frac{2}{p_j+p_k} O_{jk}|j\rangle\langle k|$, and $|j\rangle$ ($|k\rangle$) are eigenvectors of ρ with eigenvalues p_j (p_k)[34, 43].

For a fixed operation involving the estimation of a parameter, with the system prepared in different initial states, different final states can be typically obtained, and the best possible estimation precision represented by quantum Fisher information is usually different. Since the quantum Fisher information places the upper bound on the estimation precision, it can be used to characterize the power of an algorithm for estimating the parameter. We implement the DQC1 algorithm to estimate the hyperfine coupling A. By varying the degree of purity α of the control qubit, we obtain different output states. The corresponding quantum Fisher information differs, suggesting that different algorithm power leads to different estimation precision. Thus, we analyze the relationship between the quantum Fisher information and generated quantum discord to further demonstrate the role of quantum discord in the algorithm.

Fig. 5 shows the result of calculated quantum Fisher information with quantum discord in practical implementation of the algorithm to estimate the hyperfine coupling A. The quantum Fisher information presents an increasing function as the quantum discord increases, implying that larger amounts of quantum discord can lead to a more precise estimation. This supports the potential role of quantum discord as a resource in DQC1 from another perspective. The theoretical prediction is calculated without considering the interaction of system with the environment. Although the interaction causes decay on the quantum Fisher information and quantum discord, surprisingly it has little effect on their relative relationship. This may imply some intrinsic feature responsible for the successful implementation of the algorithm under such noisy environment.

In conclusion, a DQC1 algorithm has been realized on an ESR architecture with the E_2' center in α-quartz. The E_2' center provides not only an electron and nuclear spin as the con-

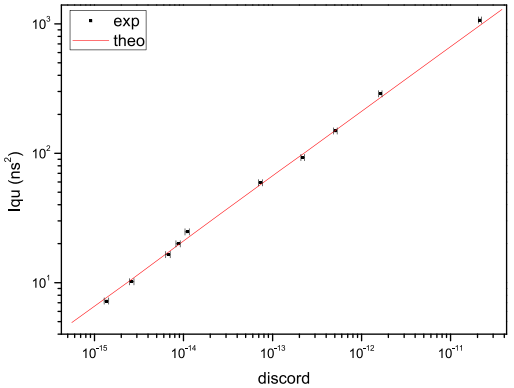

Fig. 5. Quantum Fisher information with quantum discord when implementing the DQC1 algorithm to estimate the hyperfine coupling A. Theoretical predictions are calculated without considering the interaction between the system and environment. Owing to the interaction, the experimental data for quantum Fisher information and quantum discord are much smaller than the corresponding theoretical values. However, their experimentally obtained relationship is in good agreement with the theoretical prediction as shown in the figure. The error bars only include the estimated errors in numerically calculating quantum discord with density matrices.

DOI: 10.52396/JUSTC-2021-0267
JUSTC, **2022**, 52(4): 2

trol and register qubits of the algorithm, but also a real noisy environment. This allows us to investigate quantum discord in the practical implementation of the algorithm rather than in the realization of the ideal model. Such an investigation is valuable since in practical applications of DQC1, qubits generally interact with the environment. In our case, the interaction with the environment causes a decay of quantum discord. Nevertheless, nonzero quantum discord is observed when $\theta \neq k\pi$ with integer k, confirming that quantum discord is generated in DQC1 even in a noisy environment. Furthermore, we detect the quantum discord generated with different degrees of purity α of the control qubit. α reflects the power of the DQC1 algorithm because a smaller value of α requires more runs of the algorithm for a fixed precision in estimating the normalized trace. Our results show that the value of quantum discord corresponds to the value of α, suggesting that a more powerful algorithm generates larger amounts of quantum discord in this case. We further implement the algorithm from a more practical perspective for estimating the hyperfine coupling A of the electron and nuclear spin. Quantum Fisher information presents the best possible precision of the estimation, and thereby representing the power of the algorithm. Different values of α lead to different output states wherein the measurement provides a different estimation precision of A. We have analyzed the quantum Fisher information and quantum discord for different values of α. The quantum Fisher information increases as the quantum discord increases, implying that quantum discord is helpful to advance estimation precision. All the results provide evidence of the role of quantum discord as a resource in DQC1.

Acknowledgements

The work is supported by the funding provided by the Educational Commission of Hubei Province (B2020298), the Natural Science Foundation of Hubei Province (2021CFB212), and the Youth Innovation Promotion Association of Chinese Academy of Sciences.

Conflict of interest

The authors declare that they have no conflict of interest.

Biographies

Tingwei Li is a postgraduate student at the University of Science and Technology of China. His research focuses on quantum information and quantum computation.

Fangzhou Jin is a teacher at Wuchang Shouyi University. He received his PhD from the University of Science and Technology of China in 2016. His research interests includes quantum control and quantum simulation of spin system.

Xing Rong is a Professor at the University of Science and Technology of China (USTC). He received a BS in 2005 and a PhD in 2011 from USTC. In 2014, he joined the Department of Modern Physics of USTC as a Professor. His research interest includes quantum control of spins in solids, quantum computation, and exploring new physics beyond the standard model with micrometer scale.

References

[1] Shor P. Proceedings of the 35th Annual Symposium on the Foundations of Computer Science. Washington, D.C.: IEEE, 1994.
[2] Galindo A, Martin-Delgado M A. Information and computation: Classical and quantum aspects. *Reviews of Modern Physics,* **2002**, *74* (2): 347.
[3] Goettems E I, Maciel T O, Soares-Pinto D O, et al. Promoting quantum correlations in deterministic quantum computation with a one-qubit model via postselection. *Physical Review A,* **2021**, *103* (4): 042416.
[4] Göktaş O, Tham W K, Bonsma-Fisher K, et al. Benchmarking quantum processors with a single qubit. *Quantum Information Processing,* **2020**, *19*: 146.
[5] Zhang K, Thompson J, Zhang X, et al. Modular quantum computation in a trapped ion system. *Nature Communications,* **2019**, *10* (1): 1–6.
[6] Krzyzanowska K, Copley-May M, Romain R, et al. Quantum-enhanced protocols with mixed states using cold atoms in dipole traps. *Journal of Physics: Conference Series,* **2017**, *793* (1): 012015.
[7] Pg S, Varikuti N D, Madhok V. Exponential speedup in measuring out-of-time-ordered correlators and gate fidelity with a single bit of quantum information. *Physics Letters A,* **2021**, *397*: 127257.
[8] Knill E, Laflamme R. Power of one bit of quantum information. *Physical Review Letters,* **1998**, *81* (25): 5672.
[9] Jozsa R, Linden N. On the role of entanglement in quantum-computational speed-up. *Proceedings of the Royal Society of London. Series A: Mathematical, Physical and Engineering Sciences,* **2003**, *459* (2036): 2011–2032.
[10] Horodecki R, Horodecki P, Horodecki M, et al. Quantum entanglement. *Reviews of Modern Physics,* **2009**, *81* (2): 865–942.
[11] Datta A, Flammia S T, Caves C M. Entanglement and the power of one qubit. *Physical Review A,* **2005**, *72* (4): 042316.
[12] Boyer M, Brodutch A, Mor T. Entanglement and deterministic quantum computing with one qubit. *Physical Review A,* **2017**, *95* (2): 022330.
[13] Bennett C H, DiVincenzo D P, Fuchs C A, et al. Quantum nonlocality without entanglement. *Physical Review A,* **1999**, *59* (2): 1070.
[14] Modi K, Brodutch A, Cable H, et al. The classical-quantum boundary for correlations: Discord and related measures. *Reviews of Modern Physics,* **2012**, *84* (4): 1655.
[15] Hu M L, Hu X, Wang J, et al. Quantum coherence and geometric quantum discord. *Physics Reports,* **2018**, *762*: 1–100.
[16] Bera A, Das T, Sadhukhan D, et al. Quantum discord and its allies: A review of recent progress. *Reports on Progress in Physics,* **2017**, *81* (2): 024001.
[17] Datta A, Shaji A, Caves C M. Quantum discord and the power of one qubit. *Physical Review Letters,* **2008**, *100* (5): 050502.
[18] Madsen L S, Berni A, Lassen M, et al. Experimental investigation of the evolution of Gaussian quantum discord in an open system. *Physical Review Letters,* **2012**, *109* (3): 030402.
[19] Radhakrishnan C, Lauriere M, Byrnes T. Multipartite generalization of quantum discord. *Physical Review Letters,* **2020**, *124* (11): 110401.
[20] Hunt M A, Lerner I V, Yurkevich I V, et al. How to observe and quantify quantum-discord states via correlations. *Physical Review A,* **2019**, *100* (2): 022321.
[21] Faba J, Martín V, Robledo L. Two-orbital quantum discord in fermion systems. *Physical Review A,* **2021**, *103* (3): 032426.
[22] Gu M, Chrzanowski H M, Assad S M, et al. Observing the operational significance of discord consumption. *Nature Physics,* **2012**, *8* (9): 671–675.
[23] Dakić B, Lipp Y O, Ma X, et al. Quantum discord as resource for remote state preparation. *Nature Physics,* **2012**, *8* (9): 666–670.
[24] Lanyon B P, Barbieri M, Almeida M P, et al. Experimental quantum

DOI: 10.52396/JUSTC-2021-0267
JUSTC, **2022**, 52(4): 2

computing without entanglement. *Physical Review Letters,* **2008**, *101* (20): 200501.
[25] Passante G, Moussa O, Trottier D A, et al. Experimental detection of nonclassical correlations in mixed-state quantum computation. *Physical Review A,* **2011**, *84* (4): 044302.
[26] Hor-Meyll M, Tasca D S, Walborn S P, et al. Deterministic quantum computation with one photonic qubit. *Physical Review A,* **2015**, *92* (1): 012337.
[27] Wang W, Han J, Yadin B, et al. Witnessing quantum resource conversion within deterministic quantum computation using one pure superconducting qubit. *Physical Review Letters,* **2019**, *123* (22): 220501.
[28] Ferraro A, Aolita L, Cavalcanti D, et al. Almost all quantum states have nonclassical correlations. *Physical Review A,* **2010**, *81* (5): 052318.
[29] Cable H, Gu M, Modi K. Power of one bit of quantum information in quantum metrology. *Physical Review A,* **2016**, *93* (4): 040304.
[30] Dorner R, Clark S R, Heaney L, et al. Extracting quantum work statistics and fluctuation theorems by single-qubit interferometry. *Physical Review Letters,* **2013**, *110* (23): 230601.
[31] Ryan C A, Emerson J, Poulin D, et al. Characterization of complex quantum dynamics with a scalable NMR information processor. *Physical Review Letters,* **2005**, *95* (25): 250502.
[32] Passante G, Moussa O, Ryan C A, et al. Experimental approximation of the Jones polynomial with one quantum bit. *Physical Review Letters,* **2009**, *103* (25): 250501.
[33] Helstrom C W. Minimum mean-squared error of estimates in quantum statistics. *Physics Letters A,* **1967**, *25* (2): 101–102.
[34] Braunstein S L, Caves C M. Statistical distance and the geometry of quantum states. *Physical Review Letters,* **1994**, *72* (22): 3439.
[35] Barndorff-Nielsen O E, Gill R D. Fisher information in quantum statistics. *Journal of Physics A: Mathematical and General,* **2000**, *33* (24): 4481.
[36] Weeks R A. Paramagnetic resonance of lattice defects in irradiated quartz. *Journal of Applied Physics,* **1956**, *27* (11): 1376–1381.
[37] Weeks R A, Nelson C M. Trapped electrons in irradiated quartz and silica: II, electron spin resonance. *Journal of the American Ceramic Society,* **1960**, *43* (8): 399–404.
[38] Weeks R A. Paramagnetic spectra of E_2' centers in crystalline quartz. *Physical Review,* **1963**, *130* (2): 570.
[39] Rudra J K, Fowler W B, Feigl F J. Model for the E_2' center in alpha quartz. *Physical Review Letters,* **1985**, *55* (23): 2614.
[40] Perlson B D, Weil J A. Electron paramagnetic resonance studies of the E' centers in alpha-quartz. *Canadian Journal of Physics,* **2008**, *86* (7): 871–881.
[41] Feng P, Wang Y, Rong X, et al. Characterization of the electronic structure of E_2' defect in quartz by pulsed EPR spectroscopy. *Physics Letters A,* **2012**, *376* (32): 2195–2199.
[42] Vandersypen L M K, Chuang I L. NMR techniques for quantum control and computation. *Reviews of Modern Physics,* **2005**, *76* (4): 1037.
[43] Braunstein S L, Caves C M, Milburn G J. Generalized uncertainty relations: Theory, examples, and Lorentz invariance. *Annals of Physics,* **1996**, *247* (1): 135–173.

DOI: 10.52396/JUSTC-2021-0267
JUSTC, **2022**, 52(4): 2